crowding in the pocket of the compound and arrangement of the overall complex.

From the analysis of the crystallographic data for dinuclear copper(II) cryptate, the picture that emerges is one of a disordered carbonato bridge, with two oxygens coordinated to the Cu(II) centers. For the main component (69%) the uncoordinated carbonato oxygen is hydrogen bonded to a hydronium ion (Figure 6a), while the minor component shows the uncoordinated carbonato oxygen to be coordinated to a hydronium ion in a different position (Figure 6b). The hydronium ions are stabilized by the negative carbonato oxygens, and the water molecules involved are deprotonated (i.e. become neutral water molecules) when the carbonato oxygen is in remote positions. In other words, protonation of the water molecules to form hydrogen-bonded hydronium ions is dependent on the proximity of the negatively charged carbonato oxygen.

Finally, it should be pointed out that the Cu–O distance involving the bridging carbonate is much shorter than the Cu–O bond lengths observed for any other small anionic complexes of that type, such as those with nitrate, carbonate, acetate, and formate, suggesting compression of the coordinate bonds to the bridging carbonate and a possible reason for the disorder. Thus the more linear arrangement of the bridging carbonate in the major component, seen in Figure 6a, while preferred, involves compression that is relieved in the minor component, Figure 6b, by distortion of the orientation of the bridging carbonate.

Acknowledgment. R.M. is indebted to L'Air Liquide, S.A., Paris, France, for financial assistance. Acknowledgment is made with thanks for support of this work by the Office of Naval Research. The R3m/V single-crystal X-ray diffraction and crystallographic computing system in the Crystal and Molecular Structures Laboratory of the Department of Chemistry, Texas A&M University, was purchased with funds provided by the National Science Foundation (Grant CHE-8513273).

Supplementary Material Available: For $(MX)_3(TREN)_2 \cdot 8HBr \cdot 6H_2O$, tables of anisotropic displacement parameters and H atom coordinates and isotropic displacement parameters and, for $Cu_2(\mu\text{-}CO_3)((MX)_3(TREN)_2)(H_3O)Br_3 \cdot 3H_2O$, tables of anisotropic displacement parameters and H atom coordinates and isotropic displacement parameters (8 pages); tables of structure factors for both compounds (40 pages). Ordering information is given on any current masthead page.

(36) Thompson, L. K.; Hanson, A. W.; Ramaswamy, B. S. *Inorg. Chem.* **1984**, *23*, 2459.

Contribution from the Department of Chemistry, State University of New York at Stony Brook, Stony Brook, New York 11794-3400, and Laboratoire de Chimie de Transition et de Catalyse (UA au CNRS No. 424), Institut Le Bel, Université Louis Pasteur, 4 rue Blaise Pascal, 67070 Strasbourg, France

Preparation and Structural Characterization of Dicopper(II) and Dinickel(II) Imidazolate-Bridged Macrocyclic Schiff Base Complexes

Carol A. Salata,[1a] Marie-Thérèse Youinou,*[,1b] and Cynthia J. Burrows*[,1a]

Received March 21, 1991

In order to investigate mimics of the hydrolytic enzyme urease, four new dinuclear macrocyclic complexes have been prepared by a novel template reaction, and the structure of the dicopper(II) complex with bridging imidazolate has been determined. The synthesis takes advantage of the propensity for Cu^{II} or Ni^{II} to form complexes with imidazolate. Schiff base macrocyclization of two molecules of 2,6-diacetylpyridine and two molecules of *m*-xylylenediamine occurs in the presence of 2 equiv of M^{II} and 2 equiv of ImH, leading to high yields of the dinuclear M_2(Im) complexes **1–3**. Systematic variation of anions and bridging ligands provided insight into the template synthesis process. For example, use of acetate in place of imidazolate as a bridging ligand led to formation of a dinickel complex, **4**. A crystal structure of the copper complex $[LCu_2(\mu\text{-Im})](CF_3SO_3)_3 \cdot H_2O \cdot 3THF$ (**1**) indicated a square-planar N_4 environment for each Cu with axial positions occupied by a water molecule on one Cu and two weakly bound triflates on the other Cu and showed a Cu···Cu separation of 5.92 Å. ESR and magnetic measurements of solid **1** showed antiferromagnetic coupling between the metal ions. Electrochemical studies indicated a single quasi-reversible two-electron reduction of Cu^{II} at $E_{1/2} = -435$ mV. The metal-free macrocycle was obtained by extraction of the complex with EDTA, and the $Cu_2(\mu\text{-Im})$ group could be reintroduced by addition of 2 equiv of $Cu(CF_3SO)_2$ to L in the presence of ImH. Analogous dinickel(II) complexes were prepared by the same method; spectroscopic studies indicated overall similar structures. Preliminary studies of complex **4** indicate that it acts as a modest catalyst for hydrolysis of *p*-nitrophenyl acetate.

Introduction

Synthetic dinuclear transition-metal complexes provide models for metalloprotein active sites and lend insight toward the design of new catalysts. Dinuclear complexes containing copper, iron, cobalt, and zinc have been widely studied because of their relevance to dioxygen chemistry in hemocyanin, hemerythrin, superoxide dismutase, and related proteins.[2] In contrast, models of hydrolytic metalloenzymes have primarily focused upon mononuclear species since mononuclear Zn^{II} is the most common metal center used in enzymatic hydrolysis.[3] For example, complexes of Co^{III},[4] Ni^{II},[5]

Scheme I

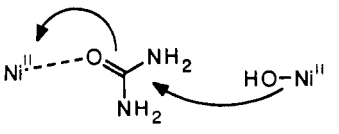

Cu^{II},[6] and Zn^{II}[7] have been shown to promote carboxylic ester and amide and phosphate ester and anhydride hydrolysis. An exception

(1) (a) State University of New York at Stony Brook. (b) Université Louis Pasteur.

(2) (a) Ibers, J. A.; Holm, R. H. *Science (Washington, D.C.)* **1980**, *209*, 223–235. (b) Que, L., Jr.; Scarrow, R. C. In *Metal Clusters in Proteins*; Que, L., Jr., Ed.; ACS Symposium Series 372; American Chemical Society: Washington, DC, 1988; pp 159–178. (c) Lippard, S. J. *Angew. Chem., Int. Ed. Engl.* **1988**, *27*, 344–361. (d) Tyeklár, Z.; Karlin, K. D. *Acc. Chem. Res.* **1989**, *22*, 241–248.

(3) (a) Christianson, D. W.; Lipscomb, W. N. *Acc. Chem. Res.* **1989**, *22*, 62–69. (b) Mathews, B. W. *Acc. Chem. Res.* **1988**, *21*, 333–340.

(4) For leading references, see: (a) Groves, J. T.; Baron, L. A. *J. Am. Chem. Soc.* **1989**, *111*, 5442–5448. (b) Chin, J.; Banaszczyk, M. *J. Am. Chem. Soc.* **1989**, *111*, 4103–4105. (c) Milburn, R. M.; Tafesse, F. *Inorg. Chim. Acta* **1987**, *135*, 119–122. (d) Schepartz, A.; Breslow, R. *J. Am. Chem. Soc.* **1987**, *109*, 1814–1826. (e) Hendry, P.; Sargeson, A. M. *J. Am. Chem. Soc.* **1989**, *111*, 2521–2527. (f) Fife, T. H.; Pujari, M. P. *J. Am. Chem. Soc.* **1988**, *110*, 7790–7797.

(5) (a) Groves, J. T.; Chambers, R. R. *J. Am. Chem. Soc.* **1984**, *106*, 630–638. (b) Blakely, R. L.; Treston, A.; Andrews, R. K.; Zerner, B. *J. Am. Chem. Soc.* **1982**, *104*, 612–614. (c) De Roach, M. A.; Trogler, W. C. *Inorg. Chem.* **1990**, *29*, 2409–2416.

0020-1669/91/1330-3454$02.50/0

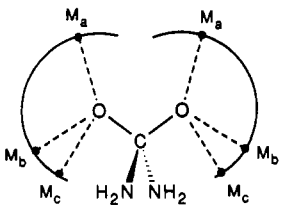

Figure 1. Proposed arrangement of metal ions around the tetrahedral intermediate of urea hydrolysis. Positions marked M_a represent a metal–metal separation of 3.4 Å as observed in (μ-acetato)dinickel complexes,[12,16] M_b represents a metal–metal separation of 5.9 Å as observed in the present work for a (μ-imidazolato)dicopper complex, and M_c represents a separation of 4.1 Å as seen in a (μ-carbonato)nickel complex.[17]

is the hydrolase purple acid phosphatase, which, from some sources, contains a dinuclear Fe–Fe or Fe–Zn center.[8] Recent magnetic measurements suggest that urease, an enzyme that enhances the rate of urea hydrolysis by a factor of 10^{14}, contains a dinuclear nickel site.[9] The Ni^{II} ions are thought to be coordinated to oxygen and/or nitrogen ligands such as imidazole in a pseudooctahedron although details of the ligand environment and internuclear Ni···Ni separation are unknown.[10] It is also not known for either of these hydrolases whether or not both metal ions participate in substrate hydrolysis. This has prompted the design and synthesis of new dinuclear complexes[11,12] including some described here which may mimic the catalytic features of urease.

In metal-catalyzed hydrolysis, two roles have been proposed for the metal ion: (i) Lewis acid activation of the carbonyl (or phosphoryl) through coordination at oxygen in order to provide a more electrophilic carbon and (ii) activation of water for nucleophilic attack by lowering its pK_a through association to the metal.[13] A mechanism put forth for urease involves both of these modes of catalysis.[14] A nickel-bound urea carbonyl could be positioned near a second nickel ion used to activate H_2O for nucleophilic attack (Scheme I).[15]

This mechanism suggests a bridging $(NH_2)_2C(O^-)_2$ group as an intermediate in urea hydrolysis and, therefore, suggests that a transition-state model should approximate this arrangement of Ni–O–C–O–Ni atoms during catalysis with the Ni···Ni separation being less than 6 Å. A range of geometries is possible for this group. Assuming an ideal tetrahedral geometry for the organic substrate (O–C–O bond angle = 109.5°; C–O bond length = 1.42 Å) and a typical M–O bond length of 2.0 Å, one can construct the model shown in Figure 1. The nickel ions should lie somewhere on hemispherical surfaces of about 2 Å radius whose projection on the O–C–O plane is given by the M_a–M_c arcs. The positions marked M_a represent a metal–metal separation of 3.4 Å. This geometry has been observed in two different dinuclear nickel complexes with bridging acetates (Ni–Ni = 3.422[12] and 3.400 Å,[16] respectively). A carbonate-bridged dinickel complex with a Ni–Ni separation of 4.1 Å has also been characterized in which each Ni^{II} coordinates in a bidentate fashion with carbonate oxygens.[17] When this structure is mapped onto the model in Figure 1, the nickel atoms occupy positions M_c.

The maximum internuclear metal–metal separation predicted by this model is 6.3 Å although such a structure would require large M–O–C bond angles. The dinuclear complexes described herein allow us to investigate metal–metal separations of about 5.9 Å (positions M_b in Figure 1).[11b] A semirigid macrocyclic ligand has been synthesized that permits dinuclear complexation of Ni^{II} or Cu^{II} while a cavity is maintained for a bridging ligand between the metal ions. The two metal-ligating sites in the macrocycle are present as 2,6-bis(iminomethyl)pyridine, and *m*-xylyl spacing groups link the two binding sites within a small range of possible M–M distances and M–X–M angles (X = bridging ligand).

Experimental Section

1. Materials. Commercial reagents were used as obtained without further purification. Propylene carbonate (PC, Merck) was dried over CaO and distilled under reduced pressure at 70 °C. Other solvents were purified and dried by standard methods before use. All reactions were commonly performed under an inert atmosphere of nitrogen.

2. Physical Measurements. IR spectra were recorded as KBr pellets on a Perkin-Elmer 1430 or a Perkin-Elmer 597 infrared spectrophotometer or a Perkin-Elmer 1600 series FT-IR instrument. Absorbances are listed in cm^{-1} as weak (w), medium (m), strong (s), shoulder (sh), or broad (br). ^1H NMR spectra were recorded on a General Electric QE-300 (300 MHz) or a Bruker SY200 (200 MHz) spectrometer. Chemical shifts (δ) are referenced to $(CH_3)_4Si$ in organic solvents. Multiplicities are as follows: s = singlet, m = multiplet, and br = broad. UV/visible spectra of solutions were obtained on a Perkin-Elmer Lambda 5 or a Cary 219 spectrophotometer with quartz cells. Elemental analyses were performed by the CNRS Microanalytical Laboratory at Lyon or Strasbourg, France, or at Galbraith Laboratories at Knoxville, TN. Mass spectra were performed in Strasbourg, France. Mass spectra requiring the chemical ionization technique were recorded on a Finnigan TFQ 70 instrument; FAB-MS was performed by using a ZAB-HF instrument from VG Analytical under positive ion conditions. Samples for FAB-MS were prepared by mixing in nitrobenzyl alcohol (NBA) containing 0.3 M toluenesulfonic acid (TSA).

The electrochemical experiments were performed at room temperature in dry propylene carbonate under O_2-free conditions by using a classical three-electrode potentiostatic setup made of a potentiostat, a pilot scanner, a current–potential converter (EDT-ECP 133), and a XY recorder (IFELEC IF 3802). The three electrodes included a hanging mercury drop electrode as the working electrode, a platinum spiral as the counter electrode and a saturated calomel electrode as reference, which was connected to the electrolysis cell by a bridge filled with a solution of tetrabutylammonium perchlorate (0.1 M) in propylene carbonate. The studies were carried out on 2×10^{-3} M solutions of the complex.

The ESR experiments were performed with a Bruker ER 420 X-band spectrometer provided with a TE_{104} cavity, a NMR gaussmeter, a frequency meter, and a BNC 12 computer for data handling facilities. The magnetic susceptibility measurements were performed with a pendulum-type magnetometer in the temperature range 4.2–150 K. Diamagnetic corrections (-630×10^{-6} cm^3 mol^{-1}) were applied for all nonmetallic atoms by using the tabulated values of Pascal's constants and refined as

(6) (a) Morrow, J. R.; Trogler, W. C. *Inorg. Chem.* **1988**, *27*, 3387–3394. (b) Morrow, J. R.; Trogler, W. C. *Inorg. Chem.* **1989**, *28*, 2330–2333. (c) Chin, J.; Jubian, V. *J. Chem. Soc., Chem. Commun.* **1989**, 839–841. (d) Duerr, B. F.; Czarnik, A. W. *Tetrahedron Lett.* **1989**, *30*, 6951–6954.

(7) (a) Woolley, P. *Nature (London)* **1975**, *258*, 677–682. (b) Fife, T. H.; Pyzystas, T. J. *J. Am. Chem. Soc.* **1986**, *108*, 4631–4636. (c) Groves, J. T.; Olson, J. R. *Inorg. Chem.* **1985**, *24*, 2715–2717. (d) Breslow, R.; Huang, D. L.; Anslyn, E. *Proc. Natl. Acad. Sci. U.S.A.* **1989**, *86*, 1746–1750, and references therein.

(8) (a) Antanaitis, B. C.; Aisen, P. *Adv. Inorg. Biochem.* **1983**, *5*, 111–136. (b) Averill, B. A.; Davis, J. C.; Burman, S.; Zirino, T.; Sanders-Loehr, J.; Loehr, T. M.; Sage, J. T.; Debrunner, P. G. *J. Am. Chem. Soc.* **1987**, *109*, 3760–3767.

(9) (a) Clark, P. A.; Wilcox, D. E. *Inorg. Chem.* **1989**, *28*, 1326–1333. (b) Clark, P. A.; Wilcox, D. E.; Scott, R. A. *Inorg. Chem.* **1990**, *29*, 579–581.

(10) (a) Andrews, R. K.; Blakeley, R. L.; Zerner, B. In *The Bioinorganic Chemistry of Nickel*; Lancaster, J. R., Jr., Ed.; VCH: New York, 1988; p 141–165. (b) Blakeley, R. L.; Treston, A.; Andrews, R. K.; Zerner, B. *J. Am. Chem. Soc.* **1982**, *104*, 612–614. (c) Dixon, N. E.; Gazzola, C.; Blakeley, R. L.; Zerner, B. *J. Am. Chem. Soc.* **1975**, *97*, 4131–4133. (d) Blakeley, R. L.; Dixon, N. E.; Zerner, B. *Biochim. Biophys. Acta* **1983**, *744*, 219–229. (e) Hasnain, S. S.; Piggott, B. *Biochem. Biophys. Res. Commun.* **1983**, *112*, 279–283.

(11) (a) Salata, C. A.; Van Engen, D.; Burrows, C. J. *J. Chem. Soc., Chem. Commun.* **1988**, 579–580. (b) Salata, C. A.; Youinou, M. T.; Burrows, C. J. *J. Am. Chem. Soc.* **1989**, *111*, 9278–9279.

(12) Buchanan, R. M.; Mashuta, M. S.; Oberhausen, K. J.; Richardson, J. R. *J. Am. Chem. Soc.* **1989**, *111*, 4497–4498.

(13) For a recent discussion with respect to carboxypeptidase A, see ref 3a.

(14) (a) Dixon, N. E.; Riddles, P. W.; Gazzola, C.; Blakeley, R. L.; Zerner, B. *Can. J. Biochem.* **1980**, *58*, 1335–1344. (b) Blakeley, R. L.; Zerner, B. *J. Mol. Catal.* **1984**, *23*, 263–292.

(15) A related mechanism has been proposed for dinuclear Co^{III}-catalyzed phosphate ester hydrolysis.[4b]

(16) Chaudhuri, P.; Küppers, H. J.; Wieghardt, K.; Gehring, S.; Haase, W.; Nuber, B.; Weiss, J. *J. Chem. Soc., Dalton Trans.* **1988**, 1367–1370.

(17) Although the third oxygen of the bridging CO_3^{2-} is not shown in Figure 1, it would lie in a position approximately midway between the two urea nitrogens shown in the figure. Mikuriya, M.; Murase, I.; Asata, E.; Kida, S. *Chem. Lett.* **1989**, 497–500.

(18) Perrin, D. D.; Armarego, W. F. L.; Perrin, D. R. *Purification of Laboratory Chemicals*; Pergamon: Oxford, England, 1980.

variable parameters in the Bleaney–Bowers equation to a value of −580 × 10^{-6} cm^3 mol^{-1}.

3. Syntheses. (a) Synthesis of $[LCu_2(\mu\text{-Im})](CF_3SO_3)_3\cdot H_2O$ (1). A solution of imidazole (104 mg, 1.53 mmol) in degassed methanol (1 mL) was mixed under nitrogen with a methanol solution (5 mL) of $Cu(OTf)_2$ (554 mg, 1.53 mmol). The resulting clear blue-green solution was added dropwise through a cannula to *m*-xylylenediamine (209 mg, 1.53 mmol) combined with 2,6-diacetylpyridine (250 mg, 1.53 mmol) in methanol (12 mL). Upon addition, the solution first turned blue and after a few minutes deep green. After the solution was stirred under nitrogen for 12 h, a fine green precipitate was obtained and isolated. Yield: 743 mg, 82%. Vapor diffusion of tetrahydrofuran into a propylene carbonate solution of the complex gave crystalline material. Anal. (crude product) Calcd for $C_{40}H_{39}N_8O_9S_3F_9Cu_2$: C, 40.50; H, 3.31; N, 9.45; Cu, 10.71. Found: C, 40.10; H, 3.39; N, 9.15; Cu, 10.46. IR (KBr pellet): ν(OH) 3460, s; ν(C=N) 1631, m; ν(phenyl) 1596, m; ν(pyridine) 1476, m; ν_{as}(SO) 1278, s (ionic CF_3SO_3); ν_{as}(SO) 1248, s (bound CF_3SO_3). Electronic spectrum (PC, λ_{max}, nm (ϵ, M^{-1} cm^{-1})): 694 (270), 294 (8700). FAB^+ MS (NBA-TSA): *m/z* 1017.0 [$(M - CF_3SO_3)^+$], 868.1 [$(M - 2CF_3SO_3)^+$], 801.0 [$(M - 2CF_3SO_3 - Im)^+$], 719.1 [$(M - 3CF_3SO_3)^+$], 652.1 [$(M - 3CF_3SO_3 - Im)^+$], 589.1 [$(M - 3CF_3SO_3 - Im - Cu)^+$]. ESR spectrum (solid state, 20 °C): $\Delta m = 2$ at $H = -1636$ G and $\Delta m = 1$ at $H = 3321$ G.

(b) Synthesis of $[LNi_2(\mu\text{-Im})](CF_3SO_3)_3\cdot 4CH_3OH$ (2). In a procedure similar to that described for $[LCu_2(\mu\text{-Im})](CF_3SO_3)_3\cdot H_2O$, a solution of imidazole (167 mg, 2.45 mmol) and $Ni(OTf)_2$ (873 mg, 2.45 mmol) was added to a solution of *m*-xylylenediamine (334 mg, 2.45 mmol) and 2,6-diacetylpyridine (400 mg, 2.45 mmol). A fine yellow precipitate was formed in a 49% yield (763 mg). Anal. Calcd for $C_{44}H_{53}N_8O_{13}S_3F_9Ni_2$: C, 41.15; H, 4.16; N, 8.72; Ni, 9.14. Found: C, 41.72; H, 4.01; N, 8.78; Ni, 8.64. IR (KBr): ν(C=N) 1620, m; ν(phenyl) 1583, m; ν(pyridine) 1461, m; ν_{as}(SO) 1279, s (ionic CF_3SO_3); ν_{as}(SO) 1250 (bound CF_3SO_3). ^1H NMR (CD_3NO_2): δ 8.53 (s, 1 H, imidazole); 8.16 (s, 2 H, imidazole). Other peaks were not attributed because of the low solubility of the compound in CD_3NO_2, which contains many impurities. FAB^+ MS (NBA-TSA): *m/z* 1155.3 (expected value = 1155.1).

(c) Synthesis of $[LiNi_2(\mu\text{-Im})](NO_3)_3\cdot 5H_2O$ (3). The previous procedure described for the copper complex was used. Addition under nitrogen of a degassed methanol solution of $Ni(NO_3)_2\cdot 6H_2O$ (891 mg, 3.1 mmol) in the presence of imidazole (209 mg, 3.1 mmol) to a solution of *m*-xylylenediamine (417 mg, 3.1 mmol) and 2,6-diacetylpyridine (500 mg, 3.1 mmol) in methanol yielded after 12 h of stirring a fine yellow precipitate, which was isolated. Yield: 955 mg, 69%. Anal. Calcd for $C_{37}H_{47}N_{11}O_{14}Ni_2$: C, 45.27; H, 4.87; N, 15.88. Found: C, 45.01; H, 4.80; N, 15.61. IR (KBr): ν(OH) 3360, br; $\nu_1(NO_3) + \nu_4(NO_3)$ 1751, w; ν(C=N) 1627, m; ν(phenyl) 1591, m; ν(pyridine) 1462, m; $\nu_3(NO_3)$ 1370, br s.

(d) Synthesis of $[LNi_2(\mu\text{-}CH_3CO_2)_x](CH_3CO_2)_{4-x}\cdot 6H_2O$ (4). In a procedure similar to that described for **1**, a degassed CH_3OH solution of $Ni(OAc)_2\cdot 4H_2O$ (153 mg, 0.61 mmol) was added to a solution of *m*-xylylenediamine (84 mg, 0.61 mmol) and 2,6-diacetylpyridine (100 mg, 0.61 mmol) in CH_3OH and stirred for 12 h. No precipitate formed, but a red-brown solid residue (207 mg) was obtained after concentration. Anal. Calcd for $C_{42}H_{58}N_6O_{14}Ni_2$: C, 51.04; H, 5.91; N, 8.50; Ni, 11.88. Found: C, 51.18; H, 5.66; N, 8.30; Ni, 12.39. IR (KBr): ν(OH) 3380, br; $\nu_{as}(CO_2)$ 1570, s; $\nu_s(CO_2)$ 1405, s; other absorptions obscured by acetate. ^1H NMR (CD_3OD): decomposition. FAB^+ MS (NBA-TSA): *m/z* 759.9 [$(M - 2CH_3CO_2)^+$], 700.8 [$(M - 3CH_3CO_2)^+$], 641.8 [$(M - 4CH_3CO_2)^+$], 583.9 [$(M - 4CH_3CO_2 - Ni)^+$].

(e) Extraction and Purification of L. To a solution of $[LCu_2(\mu\text{-Im})](CF_3SO_3)_3\cdot H_2O$ (77 mg, 0.06 mmol) in a 1/1 mixture of degassed water and benzene (total volume = 12 mL) was added under nitrogen a solution of 1 M aqueous Na_4EDTA (0.6 mL), and the resulting suspension was stirred for 10 min. The first benzene phase was removed, and because of the low solubility of the ligand, a second extraction with benzene (6 mL) was performed involving an additional 15-min period of stirring. The combined benzenic fractions were evaporated to dryness. The solid was washed with diethyl ether to remove some yellowish material, and the white powder remaining was dried under vacuum. Yield: 20 mg, 60%. The yield could eventually be improved by extracting the aqueous phase with benzene a few more times. Anal. Calcd for $C_{34}N_{34}N_6 + 0.25C_6H_6$: C, 78.04; H, 6.55; N, 15.39. Found, C, 77.46; H, 6.66; N, 14.73. IR (KBr): ν(C=N) 1632, m; ν(phenyl) 1562, m; ν(pyridine) 1445, m. ^1H NMR (C_6D_6): δ 8.30 (d, 4 H, pyr C-3 and C-5 H's); other phenyl and pyridyl proton resonances overlapped with C_6D_6 at δ 7.16, 4.81 (s, 8 H, $ArCH_2N$), 2.06 (s, 12 H, CH_3). MS (CI, isobutane) *m/z* 527.3 (expected value for $[M + H]^+$ at 527.3).

4. X-ray Crystal Structure Determination. Suitable green crystals of **1** were obtained by slow diffusion of tetrahydrofuran into a propylene carbonate solution of the complex. After 6 weeks, a crystal was selected in the mother liquor, deposited onto a cooled plate, and transferred above a liquid-nitrogen bath to a goniostat, where it was cooled to −100 °C. All data were collected on a Philips PW1100/16 diffractometer equipped with a locally built low-temperature device using nickel-filtered Cu Kα radiation (λ = 1.5418 Å). The crystal data and data collection parameters are summarized in Table II. No significant changes were observed for three standard reflections monitored every hour during the data collection period. The Enraf-Nonius SDP package[19] was used on a Microvax II computer for all the computations, except that a local data reduction program was employed. The initial step scan data were converted to intensities by the Lehmann–Larson method[20] and then corrected for Lorentz, polarization, and absorption factors, with the latter being computed by the empirical method of Wacker and Stuart.[21]

Table I. (Template)[2] Synthesis of L Using Metal Salts and Bridging Ligands[a]

entry	metal salt	bridging ligand	init product, yield[b]	L isolated[c]
1	none	none	white ppt	no
2	$Cu(OTf)_2$	none	brown residue	no
3	$Cu(OTf)_2$	imidazole	green ppt, 82%	yes
4	$Cu(OTf)_2$	pyrazole	dark blue residue	no
5	$Cu(OTf)_2$	pyrazine	dark green residue	no
6	$Cu(OTf)_2$	urea	olive green residue	no
7	$Cu(OTf)_2$	benzimidazole	dark green residue	no
8	$Cu(OAc)_2\cdot H_2O$	imidazole	dark green residue	yes
9	$Cu(OAc)_2\cdot H_2O$	(OAc^-)	dark green residue[d]	yes
10	$CuCO_3$	(CO_3^{2-})	green residue	no
11	$Ni(OTf)_2$	imidazole	light brown ppt, 49%	yes
12	$Ni(NO_3)_2\cdot 6H_2O$	imidazole	yellow ppt. 70%	yes
13	$Ni(OAc)_2\cdot 4H_2O$	imidazole	olive green residue	yes
14	$Ni(OAc)_2\cdot 4H_2O$	(OAc^-)	red-brown residue	yes
15	$NiCO_3$	(CO_3^{2-})	light green ppt	no

[a] A 1:1 ratio of metal salt and bridging ligand was used except for cases where the anion of the metal salt served as the bridging ligand (shown in parentheses). [b] If a precipitate did not form, the solution was concentrated to a solid residue and extracted with aqueous EDTA as described. [c] After extraction with EDTA; exact yields were irreproducible due to instability of L in all solvents. [d] The product slowly turned brown under N_2 and could not be further characterized.

Table II. Crystal Data, Intensity Collections, and Structure Refinement Parameters for **1**·3THF

formula	$C_{52}H_{63}N_8O_{13}S_3F_9Cu_2$
mol wt	1402.39
cryst syst	triclinic
a, Å	18.016 (6)
b, Å	18.287 (6)
c, Å	9.704 (4)
α, deg	99.99 (2)
β, deg	92.74 (2)
γ, deg	73.79 (2)
V, Å^3	3023.4
Z	2
d_{calcd}, g cm^{-3}	1.540
radiation (λ = 1.5418 Å)	Ni-filtered Cu Kα
F(000)	1444
abs coeff (μ), cm^{-1}	26.3
space group	$P\bar{1}$
cryst dimens, mm	0.300 × 0.220 × 0.080
scan mode	$\theta/2\theta$ flying step-scan
scan speed, deg $sec.^{-1}$	0.024
scan width, deg	1.0 + 0.14 tan θ
2θ range	6–104
octants	$\pm h, \pm k, +l$
no. of unique total data	8967
no. of unique obsd data	6838
criterion for observn	$I > 3\sigma(I)$
no. of variables	784
transm factors (max/min)	1.11/0.87
R_F/R_{wF}, %	4.6/6.9
GOF	1.47

(19) Frentz, B. A. In *Computing in Crystallography*; Schenk, H., Olthof-Hazekamp, R., van Koningaveld, H., Bassi, C. G., Eds.; Delft University Press: Delft, The Netherlands, 1978; pp 64–71.
(20) Lehmann, M. S.; Lansen, F. K. *Acta Crystallogr.* **1974**, *A30*, 580–584.
(21) Walker, N.; Stuart, D. *Acta Crystallogr.* **1983**, *A39*, 158–166.

The positional parameters of the copper atoms were determined by the Patterson method. The remaining non-hydrogen atoms were located on subsequent difference Fourier maps. Hydrogen atoms were introduced in structure factor calculations by their computed coordinates (C–H = 0.95 Å) and isotropic temperature factors such as $B(H) = 1 + B_{eqv}(C)$ Å^2 but not refined. Three molecules of lattice tetrahydrofuran per dinuclear complex were identified. Full least-squares refinements converged to the conventional R factors shown in Table II. Final difference maps revealed no significant maxima.

5. Hydrolysis Studies. A. Catalysis with $[LCu_2](CF_3SO_3)_4$. Solutions containing 5 mM *p*-nitrophenyl acetate or 5 mM *p*-nitrophenyl formate and 4-(2-hydroxyethyl)-1-piperazine-ethanesulfonic acid (HEPES) (0.1 M, pH 8.45) in 50% aqueous ethanol plus (a) no added catalyst, (b) 1 equiv of $Cu(OTf)_2$ added as a control study, or (c) 1 equiv of L plus 2 equiv of $Cu(OTf)_2$ as catalyst were analyzed at specific intervals by diluting an aliquot 10-fold and monitoring the absorbance at 404 nm. Studies with *p*-nitrophenyl acetate were carried out in a constant temperature bath at 25 °C; those with *p*-nitrophenyl formate were carried out at 0 °C. A_{inf} points were determined after 48 h and 30 min, respectively, at room temperature.

B. Catalysis with $[LNi_2(\mu\text{-}CH_3CO_2)_x](CH_3CO_2)_{4-x}\cdot 6H_2O$ (4). Under conditions identical with those described in part A, the hydrolysis of *p*-nitrophenyl acetate was studied at pH 8.45 and 25 °C in the presence of (a) no added catalyst, (b) 1 equiv of $Ni(CH_3CO_2)_2$ added as a control study, or (c) 1 equiv of **4** added as catalyst. Results are presented in the next section.

Results and Discussion

A. Synthesis of Dinuclear Complexes. Schiff base macrocyclization is a well-established method for preparation of mono- and dinucleating ligands from the reaction of diamines with diketones or dialdehydes. Even for dinucleating ligands, this reaction is typically performed in the presence of only a single large templating metal ion such as Pb^{2+}, Sr^{2+}, Ba^{2+}, or Ag^+.[22] In the present example, however, reaction of 2,6-diacetylpyridine with *m*-xylylenediamine in the presence of these ions failed to give the desired macrocycle and led instead to insoluble, polymeric material. This failure may be attributed to the rigidity of the linking *m*-xylyl group when compared to the more flexible polymethylenediamines commonly used.[22] It seems likely that the 24-membered macrocycle is too large, too rigid, or too poorly configured for mononuclear complexation. The use of two equivalents of $Cu(CF_3SO_3)_2$ or $Ni(CF_3SO_3)_2$ as dinuclear templates also failed to give macrocyclization (Table I, entry 2, for example). In these cases, electrostatic repulsion probably prevented the binding of M_2^{4+} in the cavity as it is being formed, and the conformation of the complex may promote oligomerization instead of ring closure.

In order to overcome the problem of electrostatic repulsion in the use of a dinuclear template, a bridging ligand was added during the synthesis of the macrocycle resulting in a dramatic increase in macrocyclization. (Compare entries 2 and 3, Table I.) Imidazole was chosen because of its well-documented ability to form μ-bridged imidazolate complexes with Cu^{II} [23] and, more rarely, with Ni^{II}.[24] In addition, the bridging N–C–N portion of imidazolate could act as a structural mimic of the O–C–O group in the urea tetrahedral intermediate, the ultimately desired substrate. In the synthesis, we postulate that imidazole serves as an initial template to first define the metal–metal separation and geometry, forming a secondary template, M–Im–M, which finally acts as a template for macrocyclization. We have termed this reaction a "(template)^2 synthesis"[11b,25] in recognition of the two-step

Scheme II

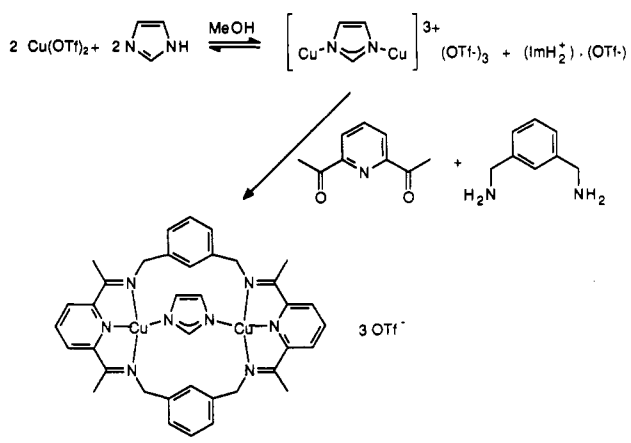

templation that precedes macrocyclization. Although the precise order of events in the mechanism cannot be determined, it is certain that both metal ions and the bridging imidazole must be present before macrocyclization will occur. Further evidence for the existence of the Cu–Im–Cu moiety prior to macrocyclization was obtained from a solution ESR spectrum at room temperature of a mixture of $Cu(CF_3SO_3)_2$ and imidazole in CH_3OH, each at a concentration of 2.5×10^{-1} M, corresponding to that used in the synthesis of **1**. Not surprisingly, such a spectrum exhibits a typical $\Delta m = 1$ transition at $g = 2.17$. However, as predicted for spin-coupled copper(II) centers, typical features are observed on each side of the resonance. Although more of a broadening is detected at low field, a distinct peak occurs at $g = 2.09$, both features being indicative of a dipole–dipole interaction. More importantly, such a drastic broadening is still observed after dilution of the methanolic copper–imidazole solution by a factor of 11. Such an observation may only be due to an intramolecular interaction, which seemingly involves imidazole as the bridging unit between two copper(II) centers during the first step of our synthesis. Thus, it seems likely that a sufficient concentration of the dinuclear template can exist, in equilibrium with other species, to serve as a template for the reaction.

In the synthetic procedure, equimolar amounts of $Cu(CF_3SO_3)_2$ or $Ni(CF_3SO_3)_2$, imidazole, diketone, and diamine in CH_3OH led to the formation of complexes **1** or **2**, respectively, after 12 h at room temperature (Scheme II). Although only 1 equiv of imidazole is required in the final complex, it is likely that a second equivalent of imidazole serves as a base for formation of the dicopper imidazolate moiety.

Not surprisingly, none of the 2 + 2 macrocyclization product, L, was obtained in the *absence* of any coordinating species (Table I, entry 1) despite other examples of high-yielding macrocyclic or macrobicyclic Schiff base syntheses.[26] In the present case, mass spectral analysis (CI, isobutane) of the organic material obtained from untemplated reactions indicates a molecular ion peak at 427.22, corresponding to a 2 + 1 product (two diketones + one diamine) with the formula $C_{26}H_{26}N_4O_2$. The presence of an intense ν(C=O) stretching absorption detected at 1695 cm^{-1} in the IR spectrum confirms the incomplete macrocyclization. Thus, the conformation of the open-chain precursor to L is inappropriate for ring closure to be competitive with polymerization. Addition of metal ions alone appears to disfavor a cyclic conformation, probably due to repulsion between the two metal cations. This repulsion is then overcome when the bridging imidazolate is present.

(22) (a) Drew, M. G. B.; Yates, P. C.; Murphy, B. P.; Nelson, J.; Nelson, S. M. *Inorg. Chim. Acta* **1986**, *118*, 37–47. (b) Abid, K. K.; Fenton, D. E. *Inorg. Chim. Acta* **1984**, *95*, 119–125. (c) Nelson, S. M. *Pure Appl. Chem.* **1980**, *52*, 2461–2476.

(23) (a) Strothkamp, K. G.; Lippard, S. J. *Acc. Chem. Res.* **1982**, *15*, 318–326. (b) Drew, M. G. B.; McCann, M.; Nelson, S. M. *J. Chem. Soc., Dalton Trans.* **1981**, 1868–1878. (c) Drew, M. G. B.; Cairns, C.; Lavery, A.; Nelson, S. M. *J. Chem. Soc., Chem. Commun.* **1980**, 1122–1124. (d) Coughlin, P. K.; Dewan, J. C.; Lippard, S. J.; Watanabe, E.; Lehn, J. M. *J. Am. Chem. Soc.* **1979**, *101*, 265–266. (e) Haddad, M. S.; Duesler, E. N.; Hendrickson, D. N. *Inorg. Chem.* **1979**, *18*, 141–148. (f) Sundberg, R. J.; Martin, R. B. *Chem. Rev.* **1974**, *74*, 471–517.

(24) Costes, J. P.; Commenges, G.; Laurent, J. P. *Inorg. Chim. Acta* **1987**, *134*, 237–244.

(25) By this definition, the formation of any such bridged dinuclear complex, M–Im–M, could be considered a template reaction since the bridge serves to orient two metal ions in defined geometries working against entropy.

(26) (a) Martell, A. E In *Advances in Supramolecular Chemistry*, Gokel, G. W., Ed.; JAI Press: Greenwich, CT, 1990; Vol. 1, pp 145–197. (b) McKee, V.; Robinson, W. T.; McDowell, D.; Nelson, J. *Tetrahedron Lett.* **1989**, *30*, 7453–7456. (c) Drew, M. G. B.; McDowell, D.; Nelson, J. *Polyhedron* **1988**, *7*, 2229–2232.

The high yields obtained for macrocyclization in the presence of imidazole suggest that the M–Im–M template is highly complementary in size and coordination geometry to the developing macrocyclic host. A variety of bridging ligands were studied with $Cu(OTf)_2$ in order to ascertain the generality of the method and the specificity of imidazole as the initial template. Pyrazole is known to have electronic properties similar to those of imidazole[27] and is believed to act as a bridging ligand, based on magnetic measurements.[28] In this case, however, addition of pyrazole did not produce L in a significant yield (Table I, entry 4). Since the pK_a's of pyrazole and imidazole are similar,[29] their different behaviors as templates must stem from either the poorer ligating ability of pyrazole[30] or from the rigidity of the *m*-xylyl groups, which do not permit contraction of the dicopper center when the shorter pyrazolate group is the bridge. Similarly, pyrazine failed to serve as an appropriate template for the reaction (Table I, entry 5). Whether this is likely due to both the increased length of the bridging ligand and its reduced stability in a [$Cu_2(\mu$-pyrazine)] complex is unknown. If the three potential bridges, pyrazole, imidazole, and pyrazine, are compared, it is clear that imidazole creates a M–L–M moiety of a shape and size most complementary to the *m*-xylyl links between binding sites. Assuming an average Cu–N bond distance of 2.0 Å, one can calculate the Cu···Cu separations and the dihedral angles between the Cu–N···N–Cu bonds to be as follows:

bridge	Cu···Cu, Å	dihedral angle, deg
pyrazine	6.8	180
imidazole	6.0	144
pyrazole	3.7	72

Since the *m*-xylylene diamine group would prefer to link the square-planar coordination geometries at an angle of about 120° and create a metal–metal separation of about 6 Å, it is most compatible with the μ-imidazolato bridge.

Urea also failed to give a good yield of the macrocycle (Table I, entry 6). Despite its inability to serve as an initial template in a dicopper system, it is still possible that once an appropriate dinuclear system is synthesized, urea could coordinate as required for catalytic hydrolysis. The more surprising failure was that of benzimidazole. The pK_a and copper coordinating ability of benzimidazole and imidazole are similar, so the explanation must rest with steric factors. One can imagine that either (i) π-stacking of benzimidazole with *m*-xylylenediamine or diacetylpyridine leads to an unfavorable conformation for ring closure or (ii) hydrogens of the benzene ring of benzimidazole interfere with other ligands on copper. Models suggest that this latter interaction may be the determining factor.

A good yield of isolated macrocycle was obtained with $Cu(OAc)_2$ with or without added imidazole. Acetate is a well-known bridging ligand in dicopper(II) complexes, so one may postulate that [$Cu_2(\mu$-$OAc)_n$] (n = 1 or 2) serves as the template for macrocyclization. (μ-Acetato)dicopper complexes typically have a Cu···Cu separation of 2.6–3.2 Å,[31] significantly shorter than what is observed here for a μ-imidazolato complex.[32] This may account for the fact that the initial copper formed in the absence of ImH (Table I, entry 9) was unstable, gradually turning brown, even under N_2. Use of $Ni(OAc)_2$ (Table I, entry 14) yielded a stable dinickel complex whose structure is postulated as [$Ni_2(\mu$-$CH_3CO_2)_x$] complex of L. (See discussion below.) Carbonate

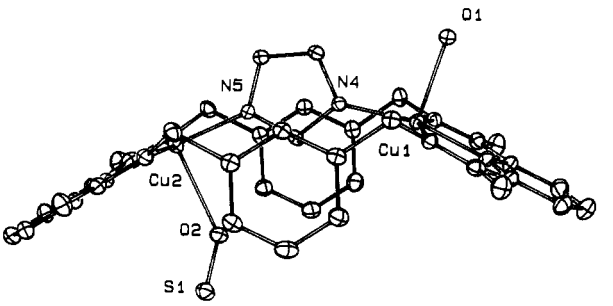

Figure 2. ORTEP drawing of **1**·3THF showing the 50% probability thermal ellipsoids. Hydrogen atoms and substituents on triflate S are omitted for clarity. Selected bond distances (Å) and angles (deg) are as follows: Cu1···Cu2 = 5.9181 (9), Cu1–N1 = 2.070 (3), Cu1–N2 = 1.928 (4), Cu1–N3 = 2.073 (3), Cu1–N4 = 1.960 (4), Cu1–O1 = 2.248 (2), Cu2–N5 = 1.945 (3), Cu2–N6 = 2.084 (3), Cu2–N7 = 1.929 (4), Cu2–N8 = 2.066 (3), Cu2–O2 = 2.442 (3), Cu2···O9 = 2.724 (4); N1–Cu1–N2 = 78.4 (1), N1–Cu1–N3 = 156.7 (1), N1–Cu1–N4 = 101.4 (1), N2–Cu1–N3 = 78.4 (1), N2–Cu1–N4 = 165.0 (1), N3–Cu1–N4 = 100.9 (1), N1–Cu1–O1 = 95.9 (1), N2–Cu1–O1 = 98.4, N7–Cu2–N8 = 78.8 (1), N6–Cu2–N8 = 155.7 (2), N5–Cu2–N8 = 102.4 (1), N6–Cu2–N7 = 78.5 (1), N5–Cu2–N7 = 177.7 (1), N5–Cu2–N6 = 100.5 (1), Cu1–N4–C37 = 128.9 (3), Cu2–N5–C37 = 126.5 (2).

was investigated as a bridging ligand; however, the very low solubility of $CuCO_3$ and $NiCO_3$ in CH_3OH yields a product corresponding to the uncyclized material of formula $C_{26}H_{26}N_4O_2$.

B. Isolation of L and Complexation Studies. The free macrocyclic ligand, L, was obtained by extraction of metals from the complexes using concentrated aqueous EDTA. During the entire extraction process, it was necessary to handle L under an inert atmosphere, and degassed solvents were used. Satisfactory results were obtained by successive extractions in benzene as the organic solvent, and C_6D_6 was also the solvent of choice for NMR spectroscopy although samples remained stable for only a few hours in benzene. Immediate decomposition of the free ligand was observed if either CH_2Cl_2 or $CHCl_3$ were used as the solvent. Macrocycle L has been thoroughly characterized. The C=N stretch appears in the normal range at 1632 cm^{-1}, and chemical ionization mass spectral analysis clearly indicated the molecular ion peak at m/z 527.3. The simplicity of the ^1H NMR spectrum of the ligand obtained from **1** reflects the high symmetry of the molecule.[33] The spectral and microanalytical data were fully consistent with the structure.

To insure that the ligand was competent for re-formation of the dinuclear complex, a titration of $Cu(OTf)_2$ into a solution of the free ligand L and imidazole in propylene carbonate was performed. The visible spectrum at λ_{max} of the complex (694 nm) was monitored and showed that 1.95 equiv of $Cu(OTf)_2$ could be titrated into the ligand/imidazole solution.

C. Characterization of 1. The green complex [$LCu_2(\mu$-Im)]$(CF_3SO_3)_3 \cdot H_2O$ (**1**) has been well characterized. The positive ion FAB mass spectrum shows the highest parent ion at m/z = 1017.0 [$(M - CF_3SO_3)^+$] with an isotropic ion distribution that closely matches the expected one. The IR spectrum of **1** shows absorptions associated with the ligand L, in particular, with the C=N stretching absorption at 1631 cm^{-1}. Water of crystallization absorbs at 3460 cm^{-1}, and the presence of coordinate triflate is evidenced by the appearance of a component of the ν(S–O) stretch below 1250 cm^{-1}.[34] Complex **1** is quite soluble in polar aprotic solvents such as propylene carbonate (PC), DMSO, and CH_3CN, and its electronic spectrum recorded in PC indicates a d–d transition at 694 nm typical of copper(II). Convincing support for the presence of a bridged imidazolate between the two coppers is given by the absence of a ν(N–H) stretching band in the IR spectrum as well as by the ESR studies: the Δm = 1 transition

(27) Johnson, C. R.; Henderson, W. W.; Shepherd, R. E. *Inorg. Chem.* **1984**, *23*, 2754–2763.
(28) (a) Robson, R. *Aust. J. Chem.* **1970**, *23*, 2217–2224. (b) Barraclough, C. G.; Brookes, R. W.; Martin, R. L. *Aust. J. Chem.* **1974**, *27*, 1843–1850. (c) Inoue, M.; Kobo, M. *J. Coord. Chem.* **1977**, *6*, 157–161. (d) Inoue, M.; Kobo, M. *Coord. Chem. Rev.* **1976**, *21*, 1–27.
(29) Yagil, G. *Tetrahedron* **1967**, *23*, 2855–2861.
(30) Bernarducci, E.; Schwindinger, W. F.; Hughey, J. L.; Krogh-Jesperson, K.; Schugar, H. J. *J. Am. Chem. Soc.* **1981**, *103*, 1686–1691.
(31) From a search of the Cambridge Crystallographic Database.
(32) On the other hand, (μ-oxalato)dicopper complexes take a form in which metal ions bind to the anti lone pairs of the carboxylates and the Cu···Cu separation is typically 5.1–5.5 Å.[31]
(33) In an earlier communication of this work,[11b] the ^1H NMR spectrum obtained in CD_2Cl_2 was misinterpreted. It is now known that free ligand L decomposes in that solvent.
(34) Dedert, P. L.; Thompson, J. S.; Ibers, J. A.; Marks, T. J. *Inorg. Chem.* **1982**, *21*, 969–977.

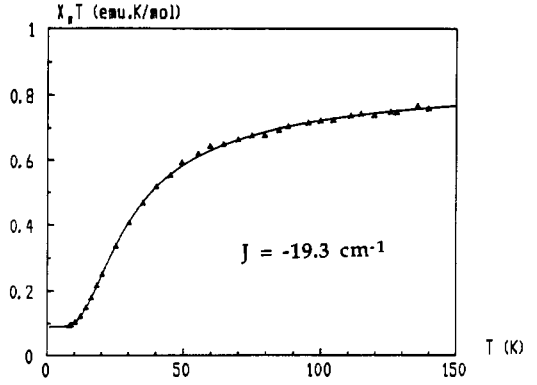

Figure 3. Magnetic susceptibility measurements of $\chi_m T$ vs T for $[Cu_2(\mu\text{-Im})L](CF_3SO_3)_3$. The solid line represents the computed fitting of the parameters as described in the text.

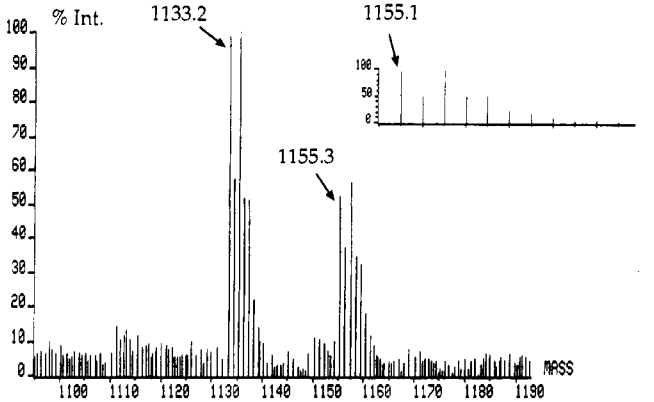

Figure 4. Mass spectrum (FAB technique) of $[LNi_2(\mu\text{-Im})](CF_3SO_3)_3$ (**2**).

at $g = 4.29$ reflects an antiferromagnetic interaction between the two Cu^{II}'s.

The crystal structure determination of **1**·3THF confirms its dimeric nature as well as the existence of a bridging imidazolate. The structure consists of discrete $[LCu_2(\mu\text{-Im})]^{3+}$ cations, triflate anions, and three independent THF molecules, with the two copper atoms located 5.92 Å apart. Figure 2 shows a perspective view of the complex cation. Each copper(II) ion is similarly coordinated to three nitrogen atoms of the macrocycle (Cu–N = 1.928 (4)–2.084 (3) Å) and to one nitrogen of the imidazolate ligand (Cu–N = 1.960 (4)–1.945 (3) Å) giving an overall square-planar N_4 environment. In addition, axial positions of both coppers are occupied by weakly coordinated H_2O (Cu1–O1 = 2.248 (2) Å) or CF_3SO_3 oxygen atoms (Cu2–O2 = 2.442 (3) Å, Cu2···O9 = 2.724 (4) Å). As expected, the copper–nitrogen bond lengths are similar for both copper sites and are close to values detected in a similar 24-membered ring complex.[23c] However, Cu1 is located further away from its mean N_4 plane (0.162 (1) Å) compared to Cu2 (–0.056 (1) Å) probably because of the absence of an extra oxygen ligand in the sixth position. Interestingly, the mean plane of the imidazolate ring lies between the phenyl rings, is almost parallel to the plane containing C9 through C14 (4 (2)° angle) and is slightly tilted at about 19.0 (4)° with respect to the second phenyl ring (involving C26 through C31). Two pyridine rings form an angle of 123.0 (2)°; a consequence of this is the feasible replacement of the imidazolate ligand by a tetrahedral intermediate, such as the group $(H_2N)_2C(O^-)_2$, implicated in catalytic hydrolysis.

The degree of interaction through the bridging imidazolate ligand is commonly depicted by the study of the magnetic susceptibility as a function of temperature. In the case of **1**, a plot of magnetic susceptibility vs temperature exhibits a maximum at 30 K and then falls to a minimum at 12 K. Such behavior is indicative of an antiferromagnetically coupled compound, associated with a small amount of paramagnetic impurity. The experimental data closely follow the Bleaney–Bowers equation,[35] giving the magnetic susceptibility as a function of temperature for a copper(II) dimer. After corrections for monomeric impurities and using values of $2N\alpha = 120 \times 10^{-6}$ cm^3 mol^{-1} and $g = 2.11$, the fitted data are represented in Figure 3, and they correspond to two weakly antiferromagnetically coupled ($S = {}^1/_2$) systems giving a singlet–triplet separation of –19.3 cm^{-1}. The magnetic exchange coupling constants in bridged imidazolate complexes have been widely studied and commonly vary from 0 to –87 cm^{-1}. Many correlations between the magnitude of the exchange coupling J and the structural parameters of the complexes have been proposed. The interaction between the two coppers through the bridging ligand can be explained in terms of a σ- and/or a π-exchange pathway. However, on the basis of theoretical calculations,[36] it has been demonstrated that a maximum value of J is obtained when the Cu–N bonds are parallel to the imidazolate carbon–carbon bond, therefore favoring a σ-exchange pathway. An increase in the Cu–N–C(Im) angles (α) and in the angle β between the vectors Cu–N(Im) should then produce a stronger coupling. Alternatively, the π-exchange pathway involves the

angle θ between the two Cu–N_4 coordination planes as well as the dihedral angle γ between the plane of the imidazole ring and the Cu–N_4 planes. In the case of complex **1** where the γ angles (93.4 (1) and 91.4 (1)°) are close to 90°, the σ-exchange pathway indeed predominates.[23a] The values of the α angles (128.9 (3) and 126.5 (2)°) and of the β angle (128, 133, and 140°, respectively, with a J value of –21.3 cm^{-1}). However, as pointed out by Lippard,[23a] the magnitude of J does not correlate strictly with the values of α in his series of bridged imidazolate complexes. Considering then the θ angle (45.2 (1)°) in **1**, larger by 3° compared to the 24-membered Schiff base complex mentioned above, and the entire series reported by Drew, Nelson, and Reedijk,[37] it seems that a correlation between J and θ cannot be excluded. One wonders, then, if the π-exchange pathway should not be included along with the σ-exchange pathway in the present case.

The electrochemical behavior of dinuclear copper complexes is to date still of interest for the understanding of type 3 copper proteins that are known to transfer two electrons in a cooperative manner. Synthetic chemists have tried to correlate the commonly observed stepwise reduction of copper(II) in dinuclear bridged systems to the nature and the length of the bridge as well as to the extent of the magnetic interaction between metal centers. So far, no definite conclusion could be drawn, although the influence of these parameters was not excluded. Recently, the importance of the cavity size of the macrocycle has been suggested as a determining factor, once the first Cu^{II} has been reduced, for the ejection of the second Cu^{I} together with the bridge ion.[38] This results in the observation of a two-step reduction at different potentials. In order to verify if a 24-membered ring was of critical size, a cyclic voltammetric study of **1** was carried out in propylene carbonate. Not surprisingly, a quasi-reversible wave at $E_{1/2} = -435$ mV was also observed, similar to that of another dinuclear complex of a Schiff base ligand,[38] and assigned to a Cu^{II}_2/Cu^{I}_2 redox process. Comparison of the height of the wave with that observed for two reference compounds[39] (assuming that their

(35) Bleaney, B.; Bowers, K. D. *Proc. R. Soc. London, A* **1952**, *214*, 451.
(36) Haddad, M. S.; Hendrickson, D. N. *Inorg. Chem.* **1978**, *17*, 2622–2630.
(37) Drew, M. G. B.; Nelson, S. M.; Reedijk, J. *Inorg. Chim. Acta* **1982**, *64*, L89–L91.
(38) Cabral, J. de O.; Cabral, M. F.; McCann, M.; Nelson, S. M. *Inorg. Chim. Acta* **1984**, *86*, L15–L18.
(39) Ferrocene as well as $[Co(tterpy)_2](PF_6)_2$ (tterpy = 4′-tolyl-2,2′:6′,2″-terpyridine),[40] the latter with properties similar to that of $[Co(terpy)_2](ClO_4)_2$ (terpy = 2,2′:6′,2″-terpyridyl),[41] were chosen for this purpose.
(40) (a) Collin, J. P.; Jouaiti, A.; Sauvage, J. P. *J. Electroanal. Chem. Interfacial Electrochem.* **1990**, *286*, 75–87. (b) Spahni, W.; Calzaferri, G. *Helv. Chim. Acta* **1984**, *67*, 450–455.

diffusion coefficients are comparable) established that the process corresponds to the transfer of two electrons.

D. Characterization of Dinickel Complexes. The (template)[2] synthetic approach led to the formation of three characterizable dinickel complexes, two containing imidazolate and one in which acetate is proposed as a bridging ligand. Crystals suitable for X-ray crystallographic analysis have not yet been obtained. The positive ion FAB mass spectrum of $[LNi_2(\mu\text{-Im})](CF_3SO_3)_3$, as shown in Figure 4, provided evidence for the analogy of this compound with the corresponding copper complex although the fragmentation pattern was not well-defined. The highest mass peak at m/z 1155.3 corresponds to the monoisotopic ion (expected value 1155.1) and shows an isotopic ion distribution pattern that is superimposable with the calculated one for the composition $C_{40}H_{37}N_8O_9S_3F_9Ni_2$. The ^1H NMR spectrum of this compound in CD_3NO_2 is quite informative about the geometry of the complex. The absence of an NH peak (as observed in imidazole alone at δ 8.36, br) as well as the observation of two singlets at δ 8.53 (1 H) and 8.16 (2 H) with a significant downfield shift compared to free imidazole (δ 7.68 (1 H) and 7.09 (2 H)) indicate coordination of imidazole to both nickels in a symmetrical fashion. More importantly, the observation of these resonances permits us to suggest the existence of a quasi-diamagnetic species in solution, although coordination of one triflate in the solid state seems to be revealed by infrared spectroscopy. Indeed, an absorption band at about 1250 cm^{-1} [35] is observed for both the dinickel complex **2** and the dicopper complex **1** whose crystal structure confirmed the weak monodentate coordination of one triflate group. The difference in coordination geometry in the solid state and solution is also supported by measurement of the magnetic moment of **2** at room temperature; the observed value of 2.99 μ_B is typical of a six-coordinate Ni^{II} environment.

By extension, the nitrate complex **3** is believed to possess the same geometry; in this case, however, the nitrate group is not coordinated as evidenced by the $\nu_3(NO_3)$ and $\nu_1(NO_3) + \nu_4(NO_3)$ bands in the infrared spectrum, neither of which show splitting.[42] The presence of a water molecule replacing the triflate group cannot be ruled out, though, since an absorption is observed at 3360 cm^{-1} and the microanalytical data would be consistent.

The geometry about nickel in the case of $[LNi_2(\mu\text{-}CH_3CO_2)_x](CH_3CO_2)_{4-x}\cdot 6H_2O$ (**4**) remains uncertain due to the lack of convenient physical methods. Problems arose because of the insolubility of the complex in common solvents and its decomposition in deuterated methanol. Therefore, the examination of its infrared spectrum was of particular importance. A typical ionic acetate group displays ν(C=O) and ν(C—O) stretching bands at 1578 and 1414 cm^{-1}. Upon coordination, the Δ value $[\nu_{as}(CO_2^-) - \nu_s(CO_2^-)]$ becomes a common criterion for determination of the mode of binding of an acetate group.[43] In the present case, the absence of a strong band at 540 cm^{-1} excludes the possibility of monodentate coordination while the Δ value of 165 cm^{-1} (absorptions at 1570 and 1405 cm^{-1}) excludes a bidentate mode (usual value of 40–80 cm^{-1}). A bridging acetate group, having a Δ value close to that of the ionic acetate group, may very well exist in complex **4** in addition to the other ionic acetate counterions. By analogy to the imidazole derivative, we suggest the formulation $[LNi_2(\mu\text{-}CH_3CO_2)_x](CH_3CO_2)_{4-x}\cdot 6H_2O$ where x = 1 or perhaps 2. The mass spectrum of **4** as well as the microanalytical data also support this conclusion. Even though the highest observed mass peak corresponds to an interaction of $(M - 2CH_3CO_2)^+$ with TSA in the matrix, the fragmentation pattern is as expected (see Experimental Section).

E. Studies of Ester Hydrolysis. Both copper and nickel complexes were studied as potential catalysts of hydrolytic reactions. Because of the difficulty of hydrolysis of urea itself, we chose as a first step to examine a readily hydrolyzed substrate, *p*-nitrophenyl acetate (AcOPNP), in order to screen the effects of several potential catalysts. The dicopper–imidazolate complex **1** was not used as a catalyst owing to complications of hydrolysis being catalyzed by free imidazole (vide infra). Rather, an analogous complex lacking the bridging imidazolate, $[LCu_2](CF_3SO_3)_4$, was prepared by addition of 2 equiv of $Cu(CF_3SO_3)_2$ to 1 equiv of L. Hydrolysis reactions were carried out with 1 equiv of metal catalyst added relative to ester substrate in pH 8.45 HEPES buffered 50% aqueous ethanol solutions at 25 °C. Table III lists the pseudo-first-order rate constants obtained for hydrolysis of *p*-nitrophenyl acetate in the absence of any catalyst (entry 1), with 2 equiv of $Cu(CF_3SO_3)_2$ added (entry 2), and with 1 equiv of $[LCu_2]^{4+}$ added (entry 3). From these data, it is evident that Cu^{2+} alone has a moderate accelerating effect on the ester hydrolysis, while addition of the ligand merely inhibits this process through complexation of the copper ions.

Table III. Pseudo-First-Order Rate Constants for the Hydrolysis of *p*-Nitrophenyl Acetate[a]

entry	catalyst	k, min^{-1}
1	none	6.0×10^{-4}
2	$Cu(CF_3SO_3)_2$	1.0×10^{-3}
3	$[LCu_2](CF_3SO_3)_4$	4.0×10^{-4}
4	$Ni(CH_3CO_2)_2$	8.1×10^{-4}
5	$[LNi_2(\mu\text{-}CH_3CO_2)_x](CH_3CO_2)_{4-x}$	5.1×10^{-3} [b]

[a] Determined at pH 8.4, HEPES buffer in 50% $EtOH/H_2O$, 25 °C. [b] Second-order rate constant; units = M^{-1} min^{-1}.

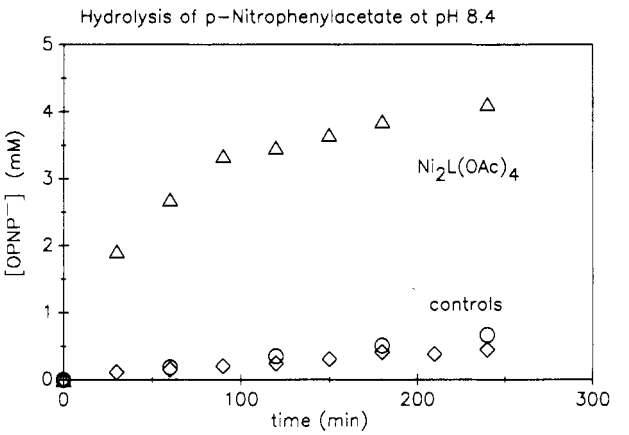

Figure 5. Kinetic studies of the influence of Ni^{II} on the rate of hydrolysis of *p*-nitrophenyl acetate. Formation of *p*-nitrophenolate was monitored at pH 8.4 for 5 mM solutions of ester containing no added metals (○), 1 equiv of $Ni(OAc)_2$ added (◇), and 1 equiv of complex **4** added (△).

Investigation of nickel complexes proved to be more interesting. The analogous $[Ni_2L]^{4+}$ complex could not be formed in the absence of bridging ligand, so complexes **2**–**4** were checked instead. Complexes **2** and **3** were somewhat unstable in 50% aqueous ethanol, leading to formation of free imidazole as determined by ^1H NMR spectroscopy. As a result, the bridging acetate complex **4** was investigated and determined to be stable for several hours in this solvent system. The results are shown in Figure 5 for the formation of $OPNP^-$ as a function of time in reactions containing (a) no catalyst, (b) 1 equiv of $Ni(CH_3CO_2)_2$, and (c) 1 equiv of $LNi_2(CH_3CO_2)_4$. Reactions a and b gave nearly identical pseudo-first-order rate constants (Table III, entries 1 and 4), indicating that Ni^{2+} in the absence of strongly coordinating ligands has no effect on the reaction rate. As is evident from Figure 5, however, complex **4** causes a dramatic increase in the formation of the reaction product, $OPNP^-$. A direct comparison cannot be made though, since this reaction shows second-order kinetics. Such an observation tells us that complex **4** is unlikely to act catalytically and must apparently be consumed, or otherwise inactivated, during the course of the reaction. Nevertheless, these observations are encouraging since the dinuclear nickel complex is clearly superior to $Ni(CH_3CO_2)_2$ in accelerating ester hydrolysis. Full characterization of the effect of the dinickel complex on ester and amide

(41) Prasad, R.; Schaife, D. B. *J. Electroanal. Chem. Interfacial Electrochem.* **1977**, *84*, 373–386.
(42) Addison, C. C.; Logan, N.; Wallwork, S. C.; Garner, C. D. *Q. Rev., Chem. Soc.* **1971**, *25*, 289–322.
(43) Nakamoto, K. *Infrared and Raman Spectra of Inorganic and Coordination Compounds*, 4th ed.; Wiley: New York, 1986, pp 231–233.

hydrolysis awaits further study.

Conclusions

A series of new dicopper(II) and dinickel(II) macrocyclic complexes have been designed as potential mimics of the dinuclear nickel enzyme urease. Their syntheses take advantage of a self-assembly process involving a dinuclear template for Schiff base macrocyclization; in the absence of the appropriate template, no macrocyclized material was formed. The [2 + 2] cyclization to form a tetraimine was found to be highly dependent upon the nature of the bridging ligand. Only imidazolate and acetate were successful with Cu^{II} and Ni^{II}. The failure of other bridging ligands in the synthetic procedure is likely due either to poor ligating ability resulting in too low a concentration of the dinuclear template or to creation of an inappropriate geometry to fit into the cavity of the developing macrocycle. These observations suggest that the method could be extended to other templated macrocyclizations with appropriate choice of the bridging ligand as a function of the cavity size and shape.

Despite the relative ease of formation of complexes **1–4**, their solution stability, and indications from the crystal structure of **1** that the macrocycle is quite strain-free, the free ligand L proved to be remarkably sensitive to decomposition in most solvents and in the solid state. One explanation might reside with the dipolar repulsion created in the free ligand upon decomplexation of the metal ions. Macrocycles containing tridentate 2,6-disubstituted pyridines often exist in the uncomplexed form with one of the substituents positioned with its lone pair directed out of the ring to relieve lone-pair repulsions with the pyridine lone pair.[11a,44] In the present case, rotation of the pyridyl–imine C–C bond might be hindered by the rigidity of the *m*-xylyl groups and thus be the source of instability of the free ligand.

The dinuclear complexes displayed spectral features typical of bridging imidazolate and bridging acetate complexes. In the case of **1**, the extent of the magnetic interaction between the two copper(II) centers was correlated to the structural parameters. The study of the magnetic properties of the dinickel bridging complexes is in progress, and their possible relevance to the urease active site would be of great interest.

A comparison of the abilities of the dicopper and dinickel complexes to promote ester hydrolysis indicated that the (μ-acetato)dinickel complex **4** holds some promise for catalytic activity, although the rate enhancement in the case studied is modest. Further refinements to the structure of the dinickel complex, notably investigation of Ni···Ni separations <6 Å, are in progress.

Acknowledgment. We thank M. Bernard and A. Derory for assistance with ESR and magnetic measurements, respectively, and Dr. J. J. Andrê and Dr. P. Legoll for fruitful discussions. The complex $[Co(tterpy)_2](PF_6)_2$ was a gift from Dr. J. P. Collin. This research was supported by a grant from the National Institutes of Health (GM-34841) to C.J.B. and a NATO Collaborative Research Grant to C.J.B. and M.-T.Y. M-T.Y. also thanks the Centre National de la Recherche Scientifique for additional support.

Supplementary Material Available: Tables of atomic coordinates and isotropic thermal parameters, bond lengths, bond angles, anisotropic thermal parameters, and hydrogen atom coordinates (15 pages). Ordering information is given on any current masthead page.

(44) Ball, P. W.; Blake, A. B. *J. Chem. Soc.* **1969**, 1415–1422.

(45) Bell, T. W.; Guzzo, F. *J. Chem. Soc., Chem. Commun.* **1986**, 769–771.

Contribution from the Department of Chemistry, University of Minnesota, Minneapolis, Minnesota 55455

Models for Catechol Dioxygenases. Structure of Bromobis[2-(2′-hydroxyphenyl)benzothiazolato]iron(III) Derived from the Bromoiron(III) Complex of 2,2′-Bis((salicylideneamino)phenyl) Disulfide

Joseph W. Pyrz, Xiangyang Pan, Doyle Britton, and Lawrence Que, Jr.*

Received February 26, 1991

The complex bromobis[2-(2-hydroxyphenyl)benzothiazolato]iron(III), $[Fe(HBT)_2Br]$ or $[Fe(C_{13}H_8NOS)_2Br]$, crystallizes in the orthorhombic space group *Pbcn* (a = 16.30 (1) Å, b = 7.666 (1) Å, c = 22.797 (9) Å, Z = 4). The crystal structure was determined at 24 °C for 2383 out of a total of 4601 reflections with R = 0.051 and R_w = 0.059. The structure reveals a trigonal-bipyramidal complex with the thiazole nitrogens in the axial positions and the phenolate oxygens and the bromide occupying the equatorial sites, structural features that are germane to the active site of the nonheme iron enzyme protocatechuate 3,4-dioxygenase. The title complex derives from an oxidative rearrangement of the bromoiron(III) complex of 2,2′-bis(salicyclideneaminophenyl) disulfide.

The catechol dioxygenases catalyze the oxidative cleavage of catechols as part of nature's mechanism for degrading aromatic molecules.[1] Protocatechuate 3,4-dioxygenase (PCD) is the best characterized of this group;[2] its crystal structure shows an active site consisting of a trigonal-bipyramidal ferric center with an axial and an equatorial tyrosine, an axial and an equatorial histidine, and a solvent molecule in an equatorial site.[3] The structure substantiates many of the active-site features that have been deduced from spectroscopic studies.[4-7] There are no model iron(III) complexes that approximate the crystallographically deduced active site. In the course of our investigations, we explored the coordination chemistry of the pentadentate ligand $salpsH_2$[8]

(1) Stanier, R. Y.; Ingraham, J. L. *J. Biol. Chem.* **1954**, *210*, 799–808. Ornston, L. N.; Stanier, R. Y. *J. Biol. Chem.* **1966**, *241*, 3776–3886.
(2) For a recent review, see: Que, L., Jr. In *Iron Carriers and Iron Proteins*; Loehr, T. M., Ed.; VCH: New York, 1989; pp 467–524.
(3) Ohlendorf, D. H.; Lipscomb, J. D.; Weber, P. C. *Nature* **1988**, *336*, 403–405.
(4) (a) Keyes, W. E.; Loehr, T. M.; Taylor, M. L. *Biochem. Biophys. Res. Commun.* **1978**, *83*, 941–945. (b) Felton, R. H.; Cheung, L. D.; Phillips, R. S.; May, S. W. *Biochem. Biophys. Res. Commun.* **1978**, *95*, 844–850. (c) Que, L., Jr.; Epstein, R. M. *Biochemistry* **1981**, *20*, 2545–2549.
(5) Whittaker, J. W.; Lipscomb, J. D. *J. Biol. Chem.* **1984**, *259*, 4487–4495.
(6) Felton, R. H.; Barrow, W. L.; May, S. W.; Sowell, A. L.; Goel, S.; Bunker, G.; Stern, E. A. *J. Am. Chem. Soc.* **1982**, *104*, 6132–6134.
(7) Pyrz, J. W.; Roe, A. L.; Stern, L. J.; Que, L., Jr. *J. Am. Chem. Soc.* **1985**, *107*, 614–620.

0020-1669/91/1330-3461$02.50/0